



Separate and independent control of interfacial band alignments and dielectric constants in transition metal rare earth complex oxides

G. Lucovsky^{a,*}, Y. Zhang^a, J.L. Whitten^b, D.G. Schlom^c, J.L. Freeouf^d

^a Department of Physics, North Carolina State University, Raleigh, NC 27695-8202, USA

^b Department of Chemistry, North Carolina State University, Raleigh, NC 27695, USA

^c Department of Materials Science, Pennsylvania State University, College Park, PA 16802, USA

^d Department of Electrical Engineering, Oregon Graduate Institute, Portland, OR 97291, USA

Abstract

Spectroscopic studies of transition metal (Tm) and rare earth (Re) oxides, combined with *ab initio* theory, identify the band edge electronic structure of alternative high-*k* dielectrics. The lowest conduction band states are derived from anti-bonding transition metal *d**-states with a π symmetry and show strong final state effects. Applied to the complex Tm/Re mixed oxides of the general form ReTmO_3 , this approach identifies a novel way for obtaining separate and independent control of band gap energies and dielectric constants through local bonding arrangements in which Tm and Re atoms are nearest neighbors to the same oxygen atom.

© 2004 Elsevier B.V. All rights reserved.

Keywords: High-*k* dielectrics; Transition metal oxides; Rare earth oxides; Complex mixed oxides

1. Introduction

The band edge electronic structure of the group IVB Tm oxides, TiO_2 , ZrO_2 , and HfO_2 , has been obtained by X-ray absorption spectroscopy (XAS) and vacuum ultra-violet spectroscopic ellipsometry (VUV SE), and coupled with *ab initio* calculations. This provides the basis for a quantitative understanding of empirically determined scaling of band

gaps and band offset energies with respect to Si as function of the atomic *d*-state energies of the respective Tm/Re atoms. Based on this scaling, and confirmed by experiment, elemental oxides, and silicate and aluminate alloys containing Sc, Ti, Ta and Nb have band offset energies too small for reducing direct tunneling to levels required for advanced devices in spite of high dielectric constants and film thickness increases of 5–10 relative to SiO_2 .

Spectroscopic studies of GdScO_3 provide an additional dimension to this scaling. Based on XAS and VUV SE measurements, and combined with an extension of *ab initio* calculations to complex oxides with Re–O–Tm bonding arrangements, it is shown that coupling of Re and Tm

* Corresponding author. Department of Electrical and Computer Engineering, North Carolina State University, Raleigh, NC 27695-8202, USA. Tel.: +1-919-515-3468; fax: +1-919-515-7331.

E-mail address: gerry_lucovsky@ncsu.edu (G. Lucovsky).

atomic d-states in these arrangements increases minimum band gaps and conduction band offset energies with respect to crystalline Si, thereby identifying novel and technologically important opportunities for band gap ‘engineering’ at the atomic scale.

2. Spectroscopic studies of group IVB Tm oxides and GdScO₃

The lowest conduction band states of ZrO₂ as determined from Zr M_{2,3} and O K₁ XAS [1] and band edge optical absorption constants from VUV SE measurements [2] are associated with symmetry-split Zr 4d*-states, and a broader band derived from Zr 5s*-states. Table 1 summarizes the relative energies of these spectral features for ZrO₂, as well as HfO₂ and TiO₂. Relative energies of these features in the X_{2,3} spectra (X = L, M, and N), normalized to the lowest d* state energy, are essentially the same for ZrO₂, HfO₂, and TiO₂ except for small differences in the d*-s* state splitting. The d*-d* and d*-s* splittings are smaller in the K₁ edge and band edge spectra as well. The d*-s* splittings are greater for TiO₂, with no d*-s* overlap in the band edge spectra, as contrasted with marked overlap for both ZrO₂ and HfO₂. Fig. 1 displays corresponding spectra for GdScO₃: the L_{2,3} spectrum for Sc in Fig. 1(a), the O K₁ edge spectrum in Fig. 1(b), the optical absorption constant in Fig. 1(c), and additional absorption edge transmission for intra 4f-level transitions in Fig. 1(d) [3]. The GdScO₃ sample is crystalline, and comparisons with the group IVB oxides are based on crystalline forms of these as well.

The features in the L_{2,3} spectrum in Fig. 1(a) are associated with localized transitions between spin-

orbit split Sc 2p_{1/2} and 2p_{3/2} states and symmetry split Sc 3d* states. Matrix element effects account for the lack of observable absorption from the Sc states to anti-bonding Sc 4s* states [4]. The spin-orbit splitting is ~4 eV, the symmetry splitting of the 3d*-states is ~2 eV, and the spectral width is <0.5 eV (the spectral resolution is ~0.2 eV).

The two features at ~532.5 and 536 eV in the O K₁ edge in Fig. 1(b) are associated with transitions to d*-states. Based on relative widths, the lower energy feature is Sc 3d*-like and the higher is Gd 5d*-like. The splitting between these states, ~3.5 eV is smaller than the splitting of ~4.2 eV in ZrO₂ (4d*) and HfO₂ (5d*), but larger than the 2.5 eV splitting in TiO₂ (3d*).

Fig. 1(c) displays the optical absorption constant, α , at the band edge as a function of photon energy obtained from the analysis of VUV SE data. The transmission measurement in Fig. 1(d) establishes that the features between about 4.8 and 5.1 eV are due to intra 4f-level transitions characteristic of the partially occupied 4f-shell in Gd [5]. The additional absorption between ~4.5 and 5.9 eV may be due to indirect band edge transitions in the GdScO₃ crystals. The rapid rise of absorption at approximately 5.8 eV in Fig. 1(c) marks the onset of transitions from the top of valence band, O 2p π non-bonding states, to the lower of the two d*-states. Since there is no distinct spectral evidence for the second d*-state, absorption above 6 eV is dominated by transitions to s*-states.

3. Ab initio calculations

The spectra for the group IVB oxides have been interpreted through ab initio calculations, the details of which will be published elsewhere [6]. The electronic structure calculations employ variational methods in which an exact Hamiltonian is used so that the variation principle applies. The calculations are done initially through a self-consistent field (SCF) Hartree-Fock calculation with a single determinant wave function, which does not include electron correlation. Following this, there is a configuration interaction (CI) refinement of the bonding orbitals based on a multi-

Table 1
Measured d*-d* and d*-s* splittings

Oxide	X _{2,3} d*-d* (d*-s*) ± 0.2 eV	K ₁ edge d*-d* (d*-s*) ± 0.2 eV	Band edge d*- d* (d*-s*) ± 0.2 eV
TiO ₂	2.0 (20)	1.8 (6)	1.4 (5)
ZrO ₂	2.4 (12)	1.3 (4.5)	~1.4 (<1)
HfO ₂	~2 (10)	1.5 (4.5)	~1.4 (<1)

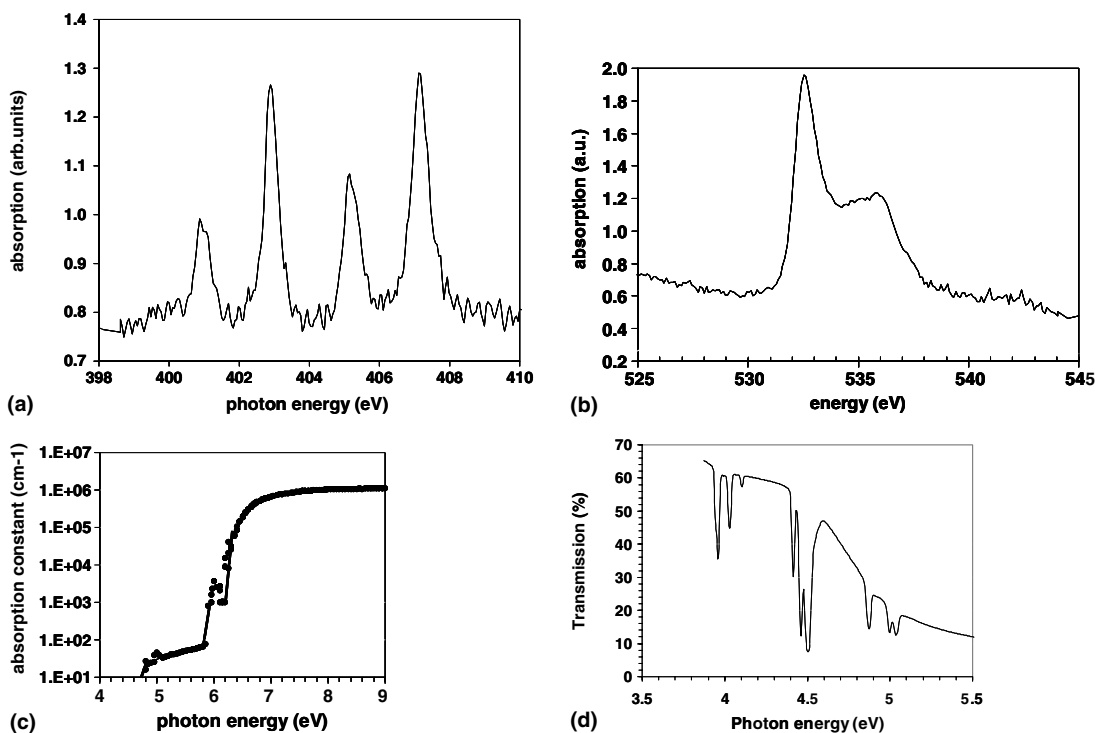


Fig. 1. GdScO_3 spectra, all plotted as functions of photon energy: (a) $L_{2,3}$ spectrum for Sc, (b) O K_1 edge spectrum, (c) band edge absorption constant, α , and (d) transmission spectrum.

determinant expansion wave function, and including electron correlation effects.

This method has been applied to small symmetric clusters that include the bonding of the transition metal atom to O neighbors terminated by H atoms with an effective charge that maintains neutrality of the cluster, while preserving the number of O neighbors, eight for Zr and Hf, and six for Ti oxide. Calculations have been made for the ground state energy, and the Zr K_1 , the Zr $M_{2,3}$, the O K_1 , and the absorption edge transitions and the corresponding electronic structures for TiO_2 , ZrO_2 , and HfO_2 . Comparisons between experimental results for relative splittings of the lowest d^* - and s^* anti-bonding states and the ab initio calculations are in excellent qualitative agreement.

Fig. 2 compares the calculated band edge electronic structures of ZrO_2 and TiO_2 . All energies are referenced to the top of the valence band, which is comprised of oxygen atom $2p \pi$ non-bonding states. Consider first the valence band states. In

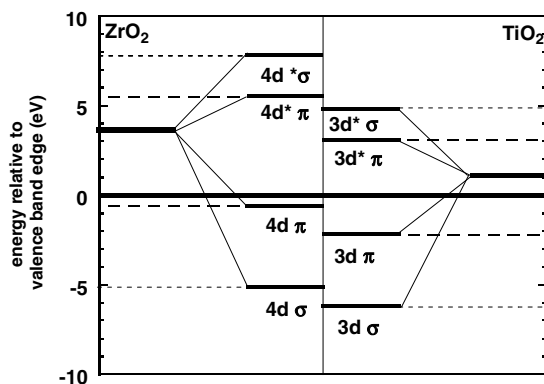


Fig. 2. Calculated band edge electronic structure of ZrO_2 and TiO_2 . Energies are referenced to the top of the valence band.

order of increasing binding energy these are non-bonding O $2p \pi$, $3d \text{ Ti}$ or $4d \text{ Zr}$ π -bonded states, and $3d \text{ Ti}$ or $4d \text{ Zr}$ σ -bonded states with the corresponding O $2p \pi$ or σ orbitals. The overlap is larger for the Ti $3d$ -O $2p \pi$ -bonding than for Zr

4d–O 2p π -bonding, hence the difference of ~ 2 eV. The differences in relative energy between the Ti 3d–O 2p and Zr 4d–O 2p σ -bonding states are similar as indicated by the dashed arrows. The separation of the conduction band d-states comes from the calculations and the relative energy of the lowest conduction band state is from experiment. The energies of the lowest Tm conduction band states have the same π^*/σ^* ordering and the energies relative to the atomic Ti 3d and Zr 4d states and are, respectively, smaller consistent with the *bonding stabilization energy* being greater than the *anti-bonding destabilization energy*.

One of the more important features of Fig. 2 is the energy difference between the respective atomic

d-states, 11.1 eV for the Ti 3d state and 8.13 for the Zr 4d state, and the respective lowest anti-bonding states. This is approximately 2 eV and is the basis for the scaling of elemental oxide band gaps with the energies of the respective atomic d-states which is displayed in Fig. 3. This explains the approximately linear dependence in the energy range between -11 and -8 eV, which includes in order of increasing (more positive) d-state energy, Ti, Nb, Ta, Sc, Zr, and Hf. The bending over at higher energies, e.g., for Y or La, is a manifestation of interactions between higher lying $(n+1)$ s^* -states, and the n $d^*-\sigma$ -state band. The flattening out at lower energy occurs for oxides of Mo and W (not high- k candidates) where d-state occupancy is increased.

Based on this scaling, and results presented in [7], the minimum band gap in GdScO_3 is expected to be determined by transitions which terminate in d^* -states with Sc 3d*-character. Since the top of the valence is O 2p p non-bonding, the valence band relative to vacuum is expected to be essentially the same in Sc_2O_3 and GdScO_3 . The band gap for Sc_2O_3 as determined from transitions terminating in the lowest lying 3d*-states is approximately 4.3 ± 0.1 eV [7], scaling arguments would place the lowest band gap in GdScO_3 at approximately the same energy, and less than 4.5 eV. This expectation is based on comparisons between the band gaps of TiO_2 and BaTiO_3 , and Nb_2O_5 and KnbO_3 [8], where the respective band gaps differ by no more than 0.2 eV.

4. Interpretation of the spectra for GdScO_3

Since the lowest band gap in GdScO_3 is at ~ 5.9 eV, this represents a marked departure from the scaling discussed above. This is accounted for by considering differences between the bonding in GdScO_3 and the elemental oxides and oxides in Fig. 4. The local bonding in GdScO_3 includes arrangements in which both Gd and Sc atoms are bonded to the same O atom. This promotes a mixing of Sc 3d-states and Gd 5d-states, which contributes to both the valence band and conduction band electronic structure. Fig. 4 presents an energy band scheme that applies. The upper

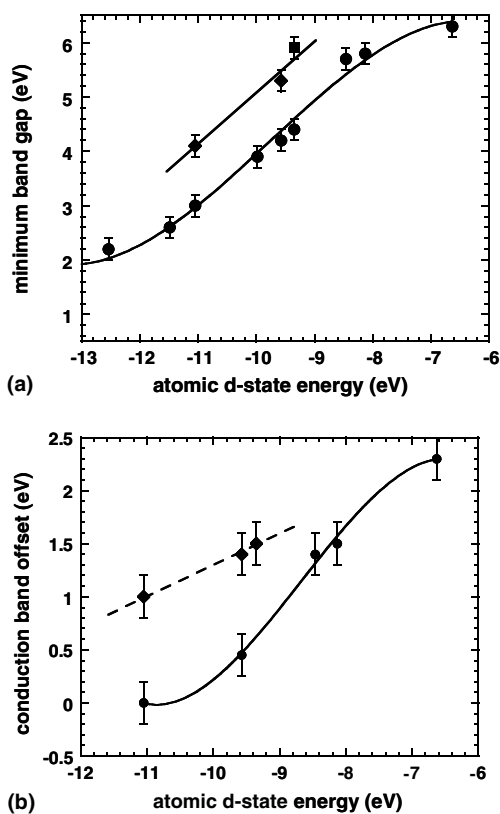


Fig. 3. (a) Empirical scaling of band gaps versus atomic d-state energy. Solid line, trend for transition metal oxides; dashed line, predicted scaling for complex oxides with d-state coupling. (b) Empirical scaling of conduction band offset energies with respect to Si versus atomic d-state energy. Solid line, trend for transition metal oxides; dashed line, predicted scaling for complex oxides with d-state coupling.

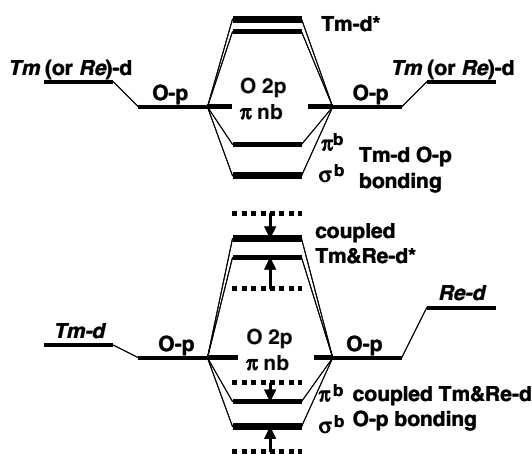


Fig. 4. Schematic representation of molecular orbitals for band edge electronic structure. Top: for elemental transition metal and rare earth oxides. Bottom: for complex oxides with d-state coupling through O-atoms.

part of the figure illustrates bonding in elemental Tm or Re oxides, e.g., Sc_2O_3 or Gd_2O_3 , in which Tm or Re atoms, respectively, are second neighbors and bonded to a common O atom. The lower portion indicates changes that occur in complex oxides in which Tm and Re atoms are second neighbors through bonding to the same O atom. For GdScO_3 , the overlap of the Sc 3d states both for π - and σ -bonding is greater than for the Gd 5d states, and this results in valence band, and antibonding states that are shifted in energy from their respective end member oxides, Sc_2O_3 and Gd_2O_3 . Based on overlap integral differences, valence band π - and σ -states are at intermediate energies with respect to the corresponding elemental oxides states. This increases the energy of the lowest conduction band state with respect to Sc_2O_3 and also makes the separation between the two d^* -states intermediate between those of a 3d-oxide and 5d-oxide. This is important for band gap/band offset energy scaling and is included in Fig. 3.

The basis for the scaling comes from comparisons between GdScO_3 and ZrO_2 , where the onsets of strong absorption occur, respectively, at 5.8 and 5.7 eV; this means that GdScO_3 has a band gap characteristic of a 4d Tm oxide. It is interesting to note that the average atomic d-state energy in GdScO_3 equals $0.5[(-6.0 \text{ eV}) + (-9.4 \text{ eV})]$ or -7.7 eV , which is close to the atomic d-state energy of ZrO_2 ,

-8.13 eV . In a similar way, the band gaps of ScO_3 , $\sim 4.5 \text{ eV}$ and Gd_2O_3 , $\sim 6.0 \text{ eV}$ average out to $\sim 5.3 \text{ eV}$. This suggests that a virtual crystal model can be applied to complex Tm/Re oxides in which d-states of the constituent atoms are coupled through bonding to common O atoms. Bonding in Tm/Re silicates and aluminates is qualitatively different and has been addressed in [1,9]. The energies of Zr core states and Si core states track across Zr silicate alloys with a constant separation [9]. This is equivalent to the difference between the band edge transitions between O 2p π non-bonding states and Zr 4d* and Si 3s* states maintaining a constant energy separation that is addressed in [1]. Tm (Re) silicate and aluminate alloys are then *two band* systems, where energies are maintained at relative end-member oxide levels, but relative absorptions change with relative concentration, whilst the complex ReTmO_3 displays a qualitatively different *single-band* behavior. Oxides with Gd_2O_3 and Sc_2O_3 , with other than the 1:1 ratio, are expected to display spectra characteristic of more than one environment; e.g., Sc_2O_3 rich alloys should display multiple d^* -state features at energies characteristic of both Sc–O–Sc and Sc–O–Gd bonding arrangements. These studies would also provide information relative to pinning down the origin of the weak absorption between about 4.5 and 5.9 eV that was previously discussed in Section 2.

5. Discussion

Fig. 4 includes the application of the virtual crystal model to complex oxides. The square point is the experimental value for GdScO_3 and is plotted at the Sc atomic d-state energy of 9.35 eV. The diamond shape point is for a HfO_2 (5d)– TiO_2 (3d), 1:1 alloy, TiHfO_4 , where the band gap is the average of HfO_2 (5.8 eV) and TiO_2 (3.1 eV) or 4.4 eV. The conduction band offset energies are estimated on the basis of the virtual crystal model. GdScO_3 is 'equivalent' to ZrO_2 with an offset of 1.5 eV, and $\text{Hf}(\text{Zr})\text{TiO}_4$ is expected to have an offset energy of approximately 1 eV, whereas a Ta_2O_5 – 2HfO_2 alloy may have an offset as high as 1.4 eV. Thin film alloys are being prepared to test these predictions of the virtual crystal model. If they prove to be

correct, then a virtual crystal behavior should occur in the dielectric constants as well, and therefore provide separate and independent control of offset energies and K . This would be particularly interesting for the TiO_2 and Ta_2O_5 complex oxides, where the dielectric constants of the elemental Tm oxides are ~ 50 and 30 , respectively.

Note added in proof

The absorption in the α -range up to $\sim 10^2 \text{ cm}^{-1}$ between about 5 eV and the rapid rise in α at the 5.8 eV band edge in Fig. 1(c), combined with the decrease in transmission beginning at $\sim 5 \text{ eV}$, and extending to the limit of the transmission measurements in Fig. 1(d) are manifestations of a reduction the symmetry at the Sc-atom and Gd-atom bonding sites. Specifically, if the local cubic or octahedral symmetries at either the Tm or Re atom bonding sites are reduced, then there will be symmetry splitting in the molecular orbitals associated with the lowest lying d^* -states and these will change the band structure in Fig. 4 by introducing a splitting of the π (and σ) d and d^* states. These will reduce the effectiveness of the coupling approach in increasing band gaps and band offset energies. Since the GdScO_3 crystal used in these spectroscopic studies had an orthorhombic crystal structure the symmetries at the Sc and Gd sites are reduced, and transitions involving d^* -states are then expected to extend below the 5.8 eV edge and down to approximately 5 eV , as in Figs. 1(c) and (d). The effect of these states on the tunneling leakage current through a reduction of the conduction band offset energy has yet to be determined. Additionally these low lying d^* -states could also introduce electron traps. Similar spectroscopic studies have been performed by our group on

HfTiO_4 , where a similar mixing of Hf $5d$ and Ti $3d$ states is expected in a crystallized compound phase [10]. XAS measurements of the O K_1 edges of HfO_2 , TiO_2 and HfTiO_4 indicate that band gap in the compound phase is not the average of the band gaps of TiO_2 and HfO_2 indicating that a similar reduction of local symmetry prevails in HfTiO_4 . The effect of the reduced band gap on direct tunneling and trapping has yet to be determined. Finally, the results for both GdScO_3 and HfTiO_4 are consistent with a dynamic Jahn-Teller effect [11].

Acknowledgements

This work is supported by the Semiconductor Research Corporation (SRC), the Office of Naval research (ONR) and the National Science Foundation (NSF).

References

- [1] G. Lucovsky, Y. Zhang, G.B. Rayner Jr., G. Appel, H. Ade, J.L. Whitten, *J. Vac. Soc. Technol. B* 20 (2002) 1739.
- [2] S.-G. Lim et al., *J. Appl. Phys.* 91 (2002) 4500.
- [3] J.H. Haeni et al., *J. Appl. Phys.*, unpublished.
- [4] E.U. Condon, G.H. Shortley, *Theory of Atomic Spectra*, Cambridge, London, 1957 (Chapter 6).
- [5] D.S. McClure, *Electronic Spectra of Molecules and Ions in Crystals*, Academic Press, New York, 1959.
- [6] G. Lucovsky, J.L. Whitten, Y. Zhang, *Solid State Electronics* 46 (2002) 1687.
- [7] H.H. Tippins, *J. Phys. Chem. Solids* 27 (1966) 1069.
- [8] P.A. Cox, *Transition Metal Oxides*, Oxford Science Publications, Oxford, 1992 (Chapter 2).
- [9] G.B. Rayner Jr., D. Kang, Y. Zhang, G. Lucovsky, *J. Vac. Sci. Technol. B* 20 (2002) 1748.
- [10] G. Lucovsky, C.C. Fulton, R.J. Nemanich, unpublished.
- [11] L. Orgel, *Introduction to Transition Metal Chemistry*, Wiley, New York, 1960.